

Substructure and the halo model of large-scale structure

Ravi K. Sheth¹ & Bhuvnesh Jain²

¹ *Department of Physics and Astronomy, University of Pittsburgh, 3941 O'Hara Street, Pittsburgh, PA 15260*

² *Department of Physics and Astronomy, University of Pennsylvania, 209 S. 33 Street, Philadelphia, PA 19104*

3 November 2018

ABSTRACT

We develop the formalism to include substructure in the halo model of clustering. Real halos are not likely to be perfectly smooth, but have substructure which has so far been neglected in the halo model — our formalism allows one to estimate the effects of this substructure on measures of clustering. We derive expressions for the two-point correlation function, the power-spectrum, the cross-correlation between galaxies and mass, as well as higher order clustering measures. Simple forms of the formulae are obtained for the limit in which the size of the substructure and mass fraction in it is small. Inclusion of substructure allows for a more accurate analysis of the statistical effects of gravitational lensing. It can also bring the halo model predictions into better agreement with the small-scale structure seen in recent high resolution simulations of hierarchical clustering.

Key words: cosmology: dark matter — cosmology: gravitational lensing — galaxies: clustering

1 INTRODUCTION

Sheth & Jain (1997) described how the halo model for clustering can allow one to model the distribution of matter in the highly nonlinear regime. The model falls within the broader framework described by Neyman & Scott (1954) and Scherrer & Bertschinger (1991). It combines results from Peebles (1974) and McClelland & Silk (1977) with the work of Press & Schechter (1974), and is able to provide a good description of nonlinear clustering seen in numerical simulations of hierarchical gravitational clustering. The halo model assumes that most of the mass in the Universe is bound up in virialized dark matter halos, and that statistical measures of clustering on small scales are dominated by the internal structure of the halos. The agreement with simulations shows that is possible to provide an accurate description of clustering in the small-scale nonlinear regime even if one has no knowledge of if and how the halos themselves are clustered. This halo-model of clustering has been the subject of much recent interest (e.g. Seljak 2000; Peacock & Smith 2000; Ma & Fry 2000; Soccimarro et al. 2001; Cooray & Sheth 2002).

To date, almost all analytic work based on the halo-model approach assumes that halos are spherically symmetric, and that the density run around each halo center is smooth. Halos which form in numerical simulations of hierarchical clustering are neither spherically symmetric nor smooth (e.g., Navarro, Frenk & White 1997; Moore et al. 1999; Jing & Suto 2002). About ten percent of the mass of a halo is associated with subclumps (Tormen, Diaferio &

Syer 1998; Ghigna et al. 1999). The main purpose of the present work is to derive a model which accounts for this substructure.

Section 2 shows how to compute two-point statistics, the correlation function and its Fourier transform, the power spectrum, when substructure is important. Section 3 shows that the model can be easily extended to estimate higher-order statistics. Section 4 shows how our formalism can incorporate a range of parent halo and subclump masses, and Section 5 provides a few explicit examples. This section includes a discussion of how to model the shape of the subclump mass function. Section 6 summarizes our results, and suggests various other applications of our formalism.

2 TWO-POINT CORRELATIONS

The halo model approach assumes that all mass is bound up in dark matter halos. All statistical measures of clustering are then decomposed into two distinct types of contributions: one comes from sets of particles which are in the same halo, and the other comes from particles which are in different halos. The assumption is that, on the smallest scales, it is the single-halo contribution which dominates the statistic. In the context of the present paper, this means that we expect that the contribution to, e.g., the power spectrum, which comes from substructure cannot be important on scales larger than a typical halo. Therefore, even if substructure changes the single-halo contribution substantially compared to the case of smooth halos, it should be accurate

to ignore substructure when estimating the two- and higher-order halo terms which dominate on larger scales. The primary consequence of substructure, then, is that the single-halo term becomes more complicated. For example, for two-point statistics, the one-halo term will now have three types of pairs: both particles from the smooth component, both particles from the substructure component, and one particle from the smooth component with the other from the substructure. Our goal will be to derive expressions for these different contributions.

2.1 Preliminaries

The probability of finding a subclump in the volume element $d^3\mathbf{r}$ at distance \mathbf{r} from the center of the parent halo of mass M is

$$p(\mathbf{r}) d^3\mathbf{r} = \frac{n_c(\mathbf{r}) d^3\mathbf{r}}{\int d^3\mathbf{r} n_c(\mathbf{r})}. \quad (1)$$

Here n_c describes the number density of subclumps at \mathbf{r} . In what follows, it will prove convenient to multiply this number density by a mass and so define a mass density ρ_c . We choose this mass so that $\int d^3\mathbf{r} \rho_c(\mathbf{r}) = M$, the total mass in the halo. (For simplicity we will sometimes assume that the subclumps have the same density run as the smooth dark matter distribution, but our analysis is not confined to this case. In this special case, ρ_c is the same as the mass density profile of the smooth component.)

The density at \mathbf{r} from the halo center is the sum of the smoothly distributed mass plus the contribution from the subclumps. If F and f_i denote the density run in units of the mean density $\bar{\rho}$ around the parent halo and the i th subclump respectively, then

$$\frac{\rho(\mathbf{r})}{\bar{\rho}} = F(\mathbf{r}) + \sum_{i=1}^N f_i(\mathbf{r} - \mathbf{r}_i). \quad (2)$$

The mass in the smooth and subclump components is defined by

$$M_s \equiv \int dr 4\pi r^2 \bar{\rho} F(r) \quad \text{and} \quad m_i \equiv \int dr 4\pi r^2 \bar{\rho} f(r). \quad (3)$$

The total mass M is the sum of the smooth and clumped components.

Our strategy will be to first derive expressions for, e.g., the correlation function for fixed values of M , m_i and N , and to average over the distributions of these variables later. We will keep the discussion as general as possible; realistic choices for F , f , p , and the halo and subclump mass functions will be inserted into the formalism later.

2.2 The correlation function of the mass

The ensemble-averaged two-point correlation function $\xi(r)$ will be obtained by averaging over halos with distributions of sub-structure specified by $p(r)$. We will first obtain the two-point correlation function within a halo, denoted $\mathcal{C}(\mathbf{r})$, then average over substructure to get $\xi(r)$, and finally in section 4 consider the averaging over varying numbers of subclumps and of parent halo masses. For a halo of total mass M we define

$$\mathcal{C}(\mathbf{r}) \equiv \bar{n} \int d^3\mathbf{s} \delta(\mathbf{s}) \delta(\mathbf{s} + \mathbf{r}), \quad \text{where} \quad \delta(\mathbf{r}) \equiv \frac{\rho(\mathbf{r})}{\bar{\rho}} - 1, \quad (4)$$

and \bar{n} denotes the number density of the parent halos. If the mass densities within the subclumps are all much larger than the mean density $\bar{\rho}$, then $\delta(\mathbf{r}) \approx \rho(\mathbf{r})/\bar{\rho}$. Writing out all the terms explicitly shows that

$$\begin{aligned} \frac{\mathcal{C}(\mathbf{r})}{\bar{n}} &= \int d^3\mathbf{s} F(\mathbf{s}) F(\mathbf{s} + \mathbf{r}) \\ &+ \sum_i \int d^3\mathbf{s} f_i(\mathbf{s} - \mathbf{r}_i) f_i(\mathbf{s} + \mathbf{r} - \mathbf{r}_i) \\ &+ \sum_j \sum_{i \neq j} \int d^3\mathbf{s} f_i(\mathbf{s} - \mathbf{r}_i) f_j(\mathbf{s} + \mathbf{r} - \mathbf{r}_j) \\ &+ \sum_i \int d^3\mathbf{s} F(\mathbf{s} + \mathbf{r}) f_i(\mathbf{s} - \mathbf{r}_i) \\ &+ \sum_i \int d^3\mathbf{s} F(\mathbf{s}) f_i(\mathbf{s} + \mathbf{r} - \mathbf{r}_i). \end{aligned} \quad (5)$$

This is the correlation function associated with a smooth component and the i subclumps at the specified positions. The first term is the contribution from particles which are not in the subclumps, and is familiar from previous work; this is the contribution from the first pair-type. The second term is from pairs where both particles are in the same subclump, whereas the third term is from pairs where the two particles are in separate subclumps. These two terms represent the contribution from the second pair-type. The fourth and fifth terms are from pairs in which one particle is in a subclump and the other is in the smoother component.

We are less interested in the correlation function associated with a specific realization of the subclump distribution, than we are with what happens upon averaging over the various possible subclump distributions. That is, we are more interested in

$$\xi(\mathbf{r}) = \int d^3\mathbf{r}_i \int d^3\mathbf{r}_j p(\mathbf{r}_i) p(\mathbf{r}_j) \mathcal{C}(\mathbf{r}). \quad (6)$$

The next step is to compute these averages.

Let $\lambda_{ss}(\mathbf{r})$ denote the value of the first integral in expression (5). It is the same for all the possible subclump distributions, so the result of averaging it over the distributions is

$$\lambda_{ss}(\mathbf{r}) = \int d^3\mathbf{s} F(\mathbf{s}) F(\mathbf{s} + \mathbf{r}). \quad (7)$$

This term is the convolution of F with itself, and is the only term which most halo-models use. The remaining terms are due to the substructure. Before we compute them, it will prove convenient to rewrite this first term as

$$\lambda_{ss}(\mathbf{r}) = \left(\frac{M_s}{M}\right)^2 \lambda_{\text{smooth}}(\mathbf{r}) = \left(1 - \sum_i \frac{m_i}{M}\right)^2 \lambda_{\text{smooth}}(\mathbf{r}).$$

Here $\lambda_{\text{smooth}}(\mathbf{r})$ denotes the correlation function if the total mass were smoothly distributed around the center of the parent halo (i.e. if there were no subclumps). Thus, the factor of $(M_s/M)^2$ simply denotes the fact that now only a fraction of the mass is in the smooth component.

Let $\lambda_{ii}(\mathbf{r})$ denote the result of averaging each of the second terms in equation (5) over $p(\mathbf{r}_i)$. Then

$$\begin{aligned}\lambda_{ii}(\mathbf{r}) &= \int d^3\mathbf{r}_i p(\mathbf{r}_i) \int d^3\mathbf{s} f_i(\mathbf{s} - \mathbf{r}_i) f_i(\mathbf{s} + \mathbf{r} - \mathbf{r}_i) \\ &= \int d^3\mathbf{x} f_i(\mathbf{x}) f_i(\mathbf{x} + \mathbf{r}),\end{aligned}\quad (8)$$

where we have set $\mathbf{x} = \mathbf{s} - \mathbf{r}_i$. This term is the convolution of each subclump profile f_i with itself.

Averaging the third term in equation (5) is more complicated so we will do it last. The result of averaging the fourth term is

$$\begin{aligned}\lambda_{si}(\mathbf{r}) &= \int d^3\mathbf{r}_i p(\mathbf{r}_i) \int d^3\mathbf{s} F(\mathbf{s} + \mathbf{r}) f_i(\mathbf{s} - \mathbf{r}_i) \\ &= \int d^3\mathbf{s} \int d^3\mathbf{r}_i f_i(\mathbf{s} - \mathbf{r}_i) F(\mathbf{s} + \mathbf{r}) \frac{\rho_c(\mathbf{r}_i)}{\int d^3\mathbf{r} \rho_c(\mathbf{r})} \\ &= \int d^3\mathbf{x} f_i(\mathbf{x}) \int d^3\mathbf{r}_i F(\mathbf{x} + \mathbf{r}_i + \mathbf{r}) \frac{\rho_c(\mathbf{r}_i)}{M} \\ &= \int \frac{d^3\mathbf{x}}{M/\bar{\rho}} f_i(\mathbf{x}) \lambda_{sc}(\mathbf{x} + \mathbf{r})\end{aligned}\quad (9)$$

where λ_{sc} denotes the convolution of F with $\rho_c/\bar{\rho}$. (If the subclumps were distributed around the halo center similarly to the dark matter, i.e., $\rho_c/\bar{\rho} \propto F$, then $\lambda_{sc} \propto \lambda_{ss}$.) By symmetry, the average of the fifth term is the same.

And finally, the average of the third term is

$$\begin{aligned}\lambda_{ij}(\mathbf{r}) &= \int d^3\mathbf{r}_i \int d^3\mathbf{r}_j p(\mathbf{r}_i) p(\mathbf{r}_j) \\ &\quad \times \int d^3\mathbf{s} f_i(\mathbf{s} - \mathbf{r}_i) f_j(\mathbf{s} + \mathbf{r} - \mathbf{r}_j),\end{aligned}\quad (10)$$

where the integral over \mathbf{s} is the convolution of the two subclump profiles. Written this way, λ_{ij} is the weighted sum of this convolution over all pairs of subclump positions. It is interesting to re-arrange the order of the integrals above:

$$\begin{aligned}\lambda_{ij}(\mathbf{r}) &= \int d^3\mathbf{r}_i \int d^3\mathbf{r}_j p(\mathbf{r}_i) p(\mathbf{r}_j) \\ &\quad \times \int d^3\mathbf{s} f_i(\mathbf{s} - \mathbf{r}_i) f_j(\mathbf{s} + \mathbf{r} - \mathbf{r}_j) \\ &= \int d^3\mathbf{s} \int d^3\mathbf{r}_i f_i(\mathbf{s} - \mathbf{r}_i) \\ &\quad \times \int d^3\mathbf{r}_j f_j(\mathbf{s} - \mathbf{r}_i + \mathbf{r} + \mathbf{r}_{ij}) p(\mathbf{r}_{ij} + \mathbf{r}_j) p(\mathbf{r}_j) \\ &= \int d^3\mathbf{x} \int d^3\mathbf{r}_{ij} f_i(\mathbf{x}) f_j(\mathbf{x} + \mathbf{r} + \mathbf{r}_{ij}) \frac{\lambda_{cc}(\mathbf{r}_{ij})}{(M/\bar{\rho})^2} \\ &= \int d^3\mathbf{x} \int d^3\mathbf{y} f_i(\mathbf{x}) f_j(\mathbf{y}) \frac{\lambda_{cc}(\mathbf{y} - \mathbf{x} - \mathbf{r})}{(M/\bar{\rho})^2}\end{aligned}\quad (11)$$

where λ_{cc} denotes the convolution of $\rho_c/\bar{\rho}$ with itself. The second line follows from setting $\mathbf{r}_{ij} = \mathbf{r}_i - \mathbf{r}_j$, the third line from setting $\mathbf{x} = \mathbf{s} - \mathbf{r}_i$ and the final expression from setting $\mathbf{y} = \mathbf{x} + \mathbf{r} + \mathbf{r}_{ij}$. When written in this way, λ_{ij} appears very similar to the two-halo term when substructure is absent; λ_{cc} plays the role of the ‘subclump–subclump correlation function’ (compare equation 2 in Sheth et al. 2001).

Using the above results, the correlation function $\xi(\mathbf{r})$ defined in equation (6) can be expressed as

$$\frac{\xi(\mathbf{r})}{\bar{n}} = \lambda_{ss}(\mathbf{r}) + \sum_i \lambda_{ii}(\mathbf{r}) + 2 \sum_i \lambda_{si}(\mathbf{r}) + \sum_i \sum_{j \neq i} \lambda_{ij}(\mathbf{r}). \quad (12)$$

Note that all the λ terms on the right-hand side have dimensions of volume, so that ξ is dimensionless.

2.3 Limiting cases for small-sized subclumps

Now consider some simple limiting cases. If the subclumps are much smaller than the parent halo, then we can treat them as point masses when performing the integrals which define λ_{si} and λ_{ij} . The associated delta function profiles simplify the integrals, so that

$$\begin{aligned}\frac{\xi(\mathbf{r})}{\bar{n}} &\approx \lambda_{ss}(\mathbf{r}) + \sum_i \lambda_{ii}(\mathbf{r}) + 2 \sum_i \frac{m_i}{M} \lambda_{sc}(\mathbf{r}) \\ &\quad + \sum_i \sum_{j \neq i} \frac{m_i}{M} \frac{m_j}{M} \lambda_{cc}(\mathbf{r}).\end{aligned}\quad (13)$$

If in addition, the distribution of subclumps around the halo center is similar to the dark matter, $\rho_c \propto F$, then we can set $\lambda_{sc} \propto \lambda_{ss}$ and $\lambda_{cc} \propto \lambda_{ss}$. In this case, the previous expression becomes

$$\begin{aligned}\frac{\xi(\mathbf{r})}{\bar{n}} &\rightarrow \lambda_{ss}(\mathbf{r}) \left[1 + 2 \sum_i \frac{m_i}{M_s} + \sum_i \sum_{j \neq i} \frac{m_i m_j}{M_s^2} \right] \\ &\quad + \sum_i \lambda_{ii}(\mathbf{r}) \\ &= \lambda_{\text{smooth}}(\mathbf{r}) \left[1 - \sum_i \left(\frac{m_i}{M} \right)^2 \right] + \sum_i \lambda_{ii}(\mathbf{r}).\end{aligned}\quad (14)$$

(Recall that λ_{smooth} denotes the correlation function if all the mass was smoothly distributed around the halo center.) If the fraction of the total mass which is in subclumps is small, then $\xi(\mathbf{r}) \approx \bar{n} \lambda_{\text{smooth}}(\mathbf{r}) + \sum_i \bar{n} \lambda_{ii}(\mathbf{r})$. In this limit, the total correlation function is well approximated by taking what one would have got if the mass was smoothly distributed, and then adding the contribution from the individual subclump components. In the small mass and size limit, the contribution from the subclumps can only be important on scales smaller than the typical subclump, so that this additional contribution is only important on very small scales. On scales larger than the diameter of a typical subclump, the correlation function looks just as though the mass within halos is smoothly distributed. This simple assumption is probably sufficiently accurate for most applications.

We remarked that the term $\lambda_{cc}(\mathbf{r})$ could be thought of as the correlation function of the subclumps. To see why, suppose there is no mass in the smooth component, and all the subclumps are infinitesimally small: i.e., we replace all factors of the subclump density profile f_i with delta functions $\delta_D(\mathbf{r}_i)$. Then, when $\mathbf{r} \neq 0$, only the third term in equation (5) contributes any pairs. Using the delta functions reduces this term to

$$\begin{aligned}\lambda_{ij}(\mathbf{r}) &= \sum_i \sum_{j \neq i} \int d^3\mathbf{r}_i \int d^3\mathbf{r}_j p(\mathbf{r}_i) p(\mathbf{r}_j) \\ &\quad \times \int d^3\mathbf{s} f_i(\mathbf{s} - \mathbf{r}_i) f_j(\mathbf{s} + \mathbf{r} - \mathbf{r}_j)\end{aligned}$$

$$= \sum_i \sum_{j \neq i} \left(\frac{m_i m_j}{\bar{\rho}^2} \right) \int d^3 \mathbf{r}_i p(\mathbf{r}_i) p(\mathbf{r}_i + \mathbf{r}), \quad (15)$$

which is proportional to the convolution of the subclump distribution ρ_c with itself.

2.4 The cross-correlation between subclumps and mass

We can use a similar argument to compute the cross correlation between subclumps and mass. That is, we imagine we sit at the center of the i th subclump and we then compute the typical density at distance \mathbf{r} from it. Because the first term in equation (5) is not centered on a subclump it no longer contributes. Since our constraint only requires one member of each pair of positions to be centered on a subclump we now need to replace one factor of f_i with a delta function. This means

$$\bar{n} \lambda_{ii}(\mathbf{r}) \rightarrow f_i(\mathbf{r}), \quad \bar{n} \lambda_{si} \rightarrow \frac{\lambda_{sc}(\mathbf{r})}{(M/\bar{\rho})}, \quad \text{and}$$

$$\bar{n} \lambda_{ij}(\mathbf{r}) \rightarrow \int d^3 \mathbf{y} f_j(\mathbf{y}) \frac{\lambda_{cc}(\mathbf{y} - \mathbf{r})}{(M/\bar{\rho})^2},$$

so that the subclump-mass cross correlation function is

$$\begin{aligned} \xi_{\times}(\mathbf{r}) &= \sum_i \frac{\lambda_{sc}(\mathbf{r})}{M/\bar{\rho}} + \sum_i f_i(\mathbf{r}) \\ &\quad + \sum_i \sum_{j \neq i} \int d^3 \mathbf{s} f_j(\mathbf{s}) \frac{\lambda_{cc}(\mathbf{s} - \mathbf{r})}{(M/\bar{\rho})^2}. \end{aligned} \quad (16)$$

In the limit in which the subclumps are much smaller in size than the parent halo the last term simplifies to give,

$$\xi_{\times}(\mathbf{r}) \approx \sum_i \frac{\lambda_{sc}(\mathbf{r})}{M/\bar{\rho}} + \sum_i f_i(\mathbf{r}) + \sum_i \sum_{j \neq i} \frac{m_j}{M} \frac{\lambda_{cc}(\mathbf{r})}{(M/\bar{\rho})}.$$

When $\rho_c/\bar{\rho} \propto F$ this becomes

$$\xi_{\times}(\mathbf{r}) \approx \sum_i \frac{\lambda_{ss}(\mathbf{r})}{M/\bar{\rho}} \left[1 + \sum_{j \neq i} \frac{m_j}{M} \right] + \sum_i f_i(\mathbf{r}), \quad (17)$$

and further, if the total mass in subclumps is small we obtain

$$\xi_{\times}(\mathbf{r}) \approx \sum_i \lambda_{ss}(\mathbf{r})/(M/\bar{\rho}) + \sum_i f_i(\mathbf{r}). \quad (18)$$

It is easy to verify that the result for ξ_{\times} can be obtained simply by averaging

$$\begin{aligned} \sum_i \rho_{cm|i}(\mathbf{r}_i + \mathbf{r}) &= \sum_i F(\mathbf{r}_i + \mathbf{r}) + \sum_i f_i(\mathbf{r}) \\ &\quad + \sum_i \sum_{j \neq i} f_j(\mathbf{r}_i + \mathbf{r} - \mathbf{r}_j) \end{aligned} \quad (19)$$

over all realizations of subclump positions, $p(\mathbf{r}_i)$ and $p(\mathbf{r}_j)$.

2.5 Power spectra

The power spectrum is the Fourier Transform of the correlation function. Since the correlation function involves a number of convolution-type integrals, the power spectrum is given by simple multiplications of the various density profile factors. Let

$$U(k) = \frac{\int dr 4\pi r^2 F(r) \sin(kr)/kr}{(2\pi)^3 \int dr 4\pi r^2 F(r)} \quad (20)$$

denote the Fourier transform of the density run of the smooth component F normalized by the total mass contained in the profile, and define $u_i(k)$ and $U_c(k)$ similarly (we have assumed we are working in three-dimensions). Then

$$\begin{aligned} P(k) &= \int \frac{dr 4\pi r^2}{(2\pi)^3} \frac{\sin(kr)}{kr} \xi(r) \\ &= \bar{n} \left(\frac{M}{\bar{\rho}} \right)^2 \left[\left(\frac{M_s}{M} \right)^2 U(k)^2 \right. \\ &\quad + 2 \sum_i \frac{m_i M_s}{M^2} u_i(k) U(k) U_c(k) \\ &\quad + \sum_i \sum_{j \neq i} \frac{m_i m_j}{M^2} u_i(k) u_j(k) U_c(k)^2 \\ &\quad \left. + \sum_i \left(\frac{m_i}{M} \right)^2 u_i(k)^2 \right], \end{aligned} \quad (21)$$

which we could write as

$$P(k) \equiv P_{ss}(k) + 2 \sum_i P_{si}(k) + \sum_i \sum_{j \neq i} P_{ij}(k) + \sum_i P_{ii}(k).$$

A similar calculation shows that the cross spectrum between subclumps and mass is

$$\begin{aligned} P_{\times}(k) &= \sum_i \left[\frac{M_s}{\bar{\rho}} U(k) U_c(k) \right. \\ &\quad \left. + U_c(k)^2 \sum_{j \neq i} \frac{m_j}{\bar{\rho}} u_j(k) + \frac{m_i}{\bar{\rho}} u_i(k) \right], \end{aligned} \quad (22)$$

and the power spectrum of the subclumps is

$$P_{cc}(k) = \bar{n} \left(\frac{M}{\bar{\rho}} \right)^2 U_c(k)^2 \sum_i \sum_{j \neq i} \frac{m_i m_j}{M M}. \quad (23)$$

If we set $U_c(k) = U(k)$, and further assume that the subclumps are much smaller than the parent halo, then the power spectrum reduces to the sum of the power spectra of the individual components:

$$\begin{aligned} \frac{P(k)}{\bar{n}} &\approx \left(\frac{M}{\bar{\rho}} \right)^2 \left[1 - \sum_i \left(\frac{m_i}{M} \right)^2 \right] U(k)^2 \\ &\quad + \sum_i \left(\frac{m_i}{\bar{\rho}} \right)^2 u_i(k)^2. \end{aligned} \quad (24)$$

This shows that whether or not the substructure component dominates the small scale power depends on the fraction of mass in the subclumps, and on how much more dense the subclumps are compared to the smooth component.

To see this a little more clearly, consider a specific example. Suppose that the density runs are Gaussians, and that all the N subclumps have the same mass m_i and size R_i . If R denotes the characteristic scale of the density runs of the smooth component, then $U = \exp(-k^2 R^2/2)$ and $u_i = \exp(-k^2 R_i^2/2)$. The subclumps dominate the power if $N(m_i/\bar{\rho})^2 u_i^2 > (M/\bar{\rho})^2 U(k)^2$. This happens on scales where $k^2 > [2 \ln(M/M_{cl}) + \ln N]/R^2/[1 - (R_i/R)^2]$, where we have set $M_{cl} \equiv N m_i$. Note that if the total mass in subclumps is

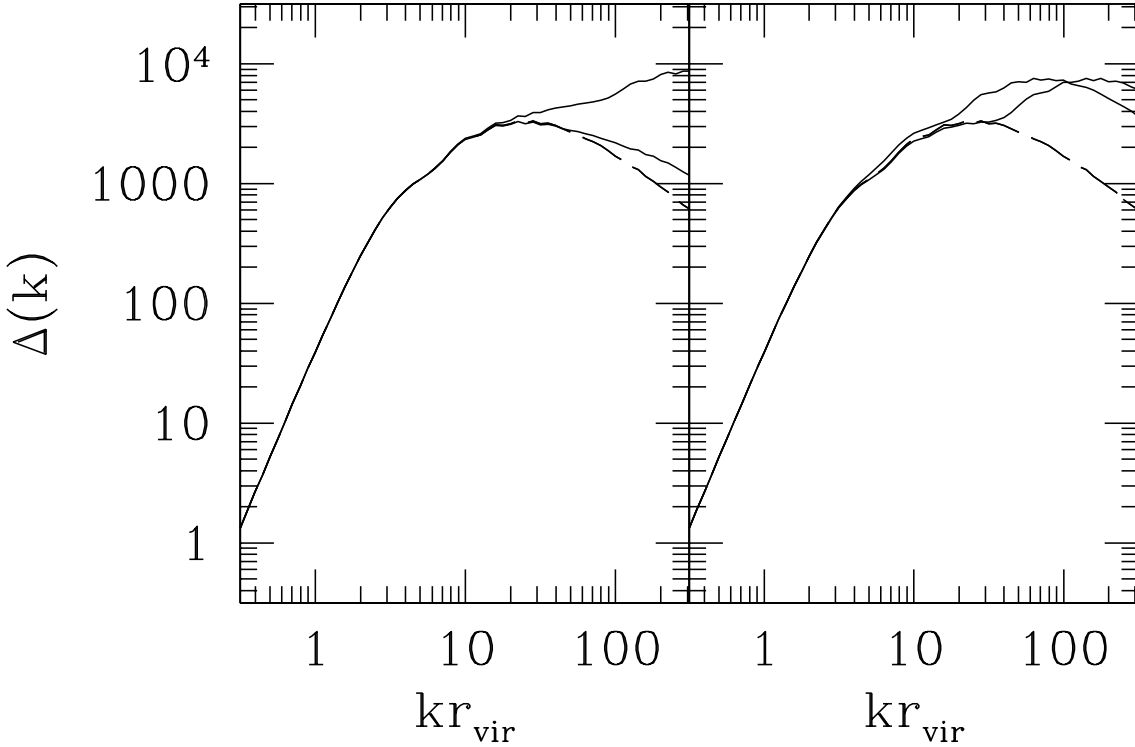


Figure 1. Effect on the power-spectrum as the parameters which describe the subclump distribution are varied. The dashed line, which is the same in both panels, shows $\Delta(k)$ when all the mass is in smooth NFW halos of radius r_{vir} within which the average density is 200 times the background density. The solid curves in the panel on the left show $\Delta(k)$ when $f = 0.1$ of the total mass of each parent halo is in subclumps, each containing 1% of the mass of the parent. The average density within each subclump is $500\bar{\rho}$ (lower) and $5000\bar{\rho}$ (higher). In the panel on the right, $f = 0.9$, the subclumps are 500 times denser than the background, and the subclumps are each 0.01 (peak at larger k) and 0.1 (peak at smaller k) times the mass of their parents.

small, $M_{\text{cl}}/M \ll 1$, then the subclumps dominate the power only at very large k ; if this mass is divided up among many subclumps, the subclumps only dominate at even higher k . For a fixed mass ratio, the exact scale on which the subclumps dominate depends on the size ratio R_i/R . This suggests that a feature in $P(k)$ at large k may provide information about the nature of the subclumps. Simulations suggest that $M/M_{\text{cl}} \sim 10$ and $R_i \lesssim R/10$, which yields a critical value of $k \gtrsim \sqrt{6 + \ln N}/R$. It is interesting that this is just beyond the reach of current simulations.

Fig. 1 illustrates this with slightly more realistic Navarro, Frenk & White (1997) density profiles. The various curves show $\Delta(k) \equiv 4\pi k^3 P(k)$ for models in which the density field is made up of Poisson distributed NFW halos. The parent halos are truncated at their virial radii r_{vir} defined so that the average density within r_{vir} is 200 times that of the background. We set the NFW core radius to be $a_{\text{NFW}} = 0.1 r_{\text{vir}}$. The dashed line (same in both panels) shows $\Delta(k)$ if there is no substructure. We then assumed that a fraction f of the mass of each parent halo was in subclumps, each of mass m . For simplicity, we assumed that the distribution of subclumps around the halo center was given by the same NFW form, and that the distribution of parti-

cles around each subclump center was also NFW, with core radius $a_{\text{NFW}} = 0.1 r_{\text{sc}}$. The value of r_{sc} was set by requiring that the average density within the subclumps equal δ_{sc} times the background density. The solid curves in the panel on the left show equation (21) when $f = 0.1$, $m = 0.01M$ and $\delta_{\text{sc}} = 500$ (lower) and $\delta_{\text{sc}} = 5000$ (upper). This shows that, all other things being equal, denser subclumps contribute more power. The solid curves in the panel on the right show results when $f = 0.9$, $\delta_{\text{sc}} = 500$ and $m/M = 0.1$ and $m/M = 0.01$ (departure from dashed curve apparent at high and still higher k). Comparison with the panel on the left shows that increasing the fraction of mass in subclumps, f , increases the small scale power. The scale on which this increase becomes apparent depends on $(m/M)^{1/3}(\delta_{\text{vir}}/\delta_{\text{sc}})^{1/3}$, the typical radii of the subclumps.

3 HIGHER-ORDER STATISTICS

Higher order correlations at a given small scale are dominated more strongly by the one-halo term than is the two point function, so the effect of substructure on the one-halo term is of great interest for higher order correlations. In this

section we will consider the effect of substructure on the 3-point correlation function. The extension to higher orders is obvious.

We begin with the expansion of the density $\rho(r)$ given in equation (2). The 3-point function in real space is then defined by

$$\xi_{123} \equiv \langle \delta(\mathbf{r}_1)\delta(\mathbf{r}_2)\delta(\mathbf{r}_3) \rangle \simeq \frac{1}{\bar{\rho}^3} \langle \rho(\mathbf{r}_1)\rho(\mathbf{r}_2)\rho(\mathbf{r}_3) \rangle. \quad (25)$$

It is convenient to consider the expressions for higher order correlations in Fourier space, since we will find that in the limiting case of interest the only additional term due to substructure is a term involving products of the substructure profile.

The Fourier transform of the 3-point function is the bispectrum B defined by

$$\langle \delta(\mathbf{k}_1)\delta(\mathbf{k}_2)\delta(\mathbf{k}_3) \rangle = B(\mathbf{k}_1, \mathbf{k}_2, \mathbf{k}_3) (2\pi)^3 \delta_D(\mathbf{k}_{123}), \quad (26)$$

where the Delta function indicates that $\mathbf{k}_1 + \mathbf{k}_2 + \mathbf{k}_3 = 0$.

It is the sum of contributions from triplets which are all in the smooth component, triplets all in the same halo, plus contributions from the various cross terms. Writing all the different terms explicitly gives

$$\begin{aligned} B(k_1, k_2, k_3) = & \bar{n} \left[\left(\frac{M_s}{\bar{\rho}} \right)^3 U(k_1)U(k_2)U(k_3) \right. \\ & + \sum_i \frac{m_i}{\bar{\rho}} u_i(k_1) \left(\frac{M_s}{\bar{\rho}} \right)^2 U(k_2)U(k_3) U_c(k_1) \\ & + \sum_i \frac{M_s}{\bar{\rho}} U(k_1) \left(\frac{m_i}{\bar{\rho}} \right)^2 u_i(k_2)u_i(k_3) U_c(k_1) \\ & + \sum_i \sum_{j \neq i} \frac{m_i m_j}{\bar{\rho}^2} u_i(k_1)u_j(k_2) \frac{M_s}{\bar{\rho}} U(k_3) U_c(k_1)U_c(k_2) \\ & + \sum_i \sum_{j \neq i} \sum_{k \neq j \neq i} \frac{m_i m_j m_k}{\bar{\rho}^3} u_i(k_1)u_j(k_2)u_k(k_3) \\ & \quad \times U_c(k_1)U_c(k_2)U_c(k_3) \\ & + \sum_i \sum_{j \neq i} \frac{m_i}{\bar{\rho}} u_i(k_1) \left(\frac{m_j}{\bar{\rho}} \right)^2 u_j(k_2)u_j(k_3) U_c(k_1)^2 \\ & \left. + \sum_i \left(\frac{m_i}{\bar{\rho}} \right)^3 u_i(k_1)u_i(k_2)u_i(k_3) \right], \quad (27) \end{aligned}$$

where $\mathbf{k}_3 = -\mathbf{k}_1 - \mathbf{k}_2$. Further integrations over appropriate window functions yield the spatially smoothed skewness (see, e.g., Scoccimarro et al. 2001; Takada & Jain 2002; Cooray & Sheth 2002). Similar relations hold for the higher order correlations.

In the same small mass and size limits which we used when studying $\xi(r)$ and $P(k)$, the bispectrum is dominated by the first and last terms of equation (27).

4 AVERAGING OVER NUMBERS AND MASSES

So far we have assumed that the masses and numbers of subclumps were fixed. This section shows the result of allowing for a distribution of masses and numbers. Expressions for the power spectra are much simpler than for $\xi(r)$, so we will

only consider $P(k)$ here. Analogously, the averaged bispectrum B is much simpler to evaluate than ξ_{123} . For what is to follow, it is useful to write explicitly that the quantity in the previous section is computed at fixed values of M , \mathcal{N} and $\mathbf{m} \equiv \{m_1, \dots, m_{\mathcal{N}}\}$, where the masses and density profiles of the \mathcal{N} subclumps may be different. The quantity we are after is

$$\int dM \frac{dN(M)}{dM} \sum p(\mathcal{N}|M) p(\mathbf{m}|\mathcal{N}, M) P(k|\mathbf{m}, \mathcal{N}, M), \quad (28)$$

where dN/dM is the number density of parent M halos (usually called the universal halo mass function), $p(\mathcal{N}|M)$ is the probability an M halo has \mathcal{N} subclumps, $p(\mathbf{m}|\mathcal{N}, M)$ is the probability that the \mathcal{N} subclumps were $\{m_1, \dots, m_{\mathcal{N}}\}$ given that there were \mathcal{N} of them in the M halo, $P(k|\mathbf{m}, \mathcal{N}, M)$ is the quantity we computed in the previous section, and the sum is over all values of \mathcal{N} and \mathbf{m} . To proceed, we need models of these different distributions.

If all the subclumps are identical, and there are \mathcal{N} of them, then each of the terms in the sums over i and j are the same, so the contribution to the power from the smooth-subclump cross-terms is \mathcal{N} times the contribution from a single clump, and the contribution from the subclump-subclump terms is $\propto \mathcal{N}(\mathcal{N} - 1) U_c^2$. In this case, the total power depends on the first two factorial moments of the $p(\mathcal{N}|M)$ distribution. If the subclumps are much smaller than their parents, then equation (24) implies that

$$\begin{aligned} P(k) \approx & \bar{n} \left(\frac{M}{\bar{\rho}} \right)^2 [1 - \mathcal{N}(m/M)^2] U(k)^2 \\ & + \mathcal{N} \bar{n} \left(\frac{m}{\bar{\rho}} \right)^2 u(k)^2. \quad (29) \end{aligned}$$

The factor $\mathcal{N}\bar{n}$ is simply the number density of the subclumps, so it may be useful to think of the two terms above separately. The first term requires knowledge of the mass function of the parent halos, whereas the second requires the ‘mass function’ of the subclumps. As discussed in Section 5, accurate formulae for the parent mass function are available; subclump mass functions are only just becoming available.

In practice, halos of the same M have different substructure distributions. For example, we expect that there will be some scatter around the mean number of subclumps $N_{cl} \equiv \langle \mathcal{N}|M \rangle$ in an M -halo, as well as in the fraction of mass associated with the clumped component: M_{cl}/M . However, if the scatter around the typical subclump configuration is small, then we should get a reasonable estimate of the effects of substructure if we use a good model of the typical configuration, and neglect the fact that there is actually some scatter around it. This is our strategy.

Let $dn(m|M)/dm$ denote the typical subclump mass function. Then

$$\begin{aligned} P(k) = & \int dM \frac{dN(M)}{dM} \left(\frac{M_s}{\bar{\rho}} \right)^2 U(k|M)^2 \\ & + 2 \int dM \frac{dN(M)}{dM} \frac{M_s}{\bar{\rho}} U(k) \\ & \times \int dm \frac{dn(m|M)}{dm} \frac{m}{\bar{\rho}} u(k|m) U_c(k|m) \end{aligned}$$

$$\begin{aligned}
 & + \int dM \frac{dN(M)}{dM} \int dm_1 \frac{dn(m_1|M)}{dm_1} \frac{m_1}{\rho} u(k|m_1, M) \\
 & \quad \times \int dm_2 \frac{dn(m_2|M, m_1)}{dm_2} \frac{m_2}{\rho} \\
 & \quad \times u(k|m_2, M, m_1) U_c(k|m_1, m_2)^2 \\
 & + \int dM \frac{dN(M)}{dM} \\
 & \quad \times dm \frac{dn(m|M)}{dm} \frac{m^2}{\rho^2} u(k|m, M)^2. \quad (30)
 \end{aligned}$$

The third term is the tricky one: it requires the joint distribution of m_1 - and m_2 -subclumps in an M -halo. Following Sheth & Lemson (1999), we have chosen to write this as the typical number of m_1 -subclumps in an M -halo times the typical number of m_2 -subclumps in M -halos which have an m_1 -subclump. Similarly, the notation $U_c(k|m_1, m_2)$ is intended to allow for the possibility that the distribution of m_2 -subclumps within the parent M -halo may depend on whether or not the parent contains an m_1 -subclump.

In the limit in which the subclumps are much smaller than the parent, and contribute a small fraction of the total mass, the expression above becomes

$$\begin{aligned}
 P(k) & \approx \int dM \frac{dN(M)}{dM} \left(\frac{M_s}{\rho} \right)^2 U(k|M)^2 \\
 & + \int dM \frac{dN(M)}{dM} \int dm \frac{dn(m|M)}{dm} \frac{m^2}{\rho^2} u(k|m, M)^2.
 \end{aligned}$$

The integral over m is from zero to M . If $u(k|m, M)$ is only a function of m (i.e., if the density profile of an m subclump is independent of the mass of the parent in which it sits), then the order of the integrals above can be rearranged. If we define the mass function of the subclumps as

$$\frac{dN_c(m)}{dm} \equiv \int_m^\infty dM \frac{dN(M)}{dM} \frac{dn(m|M)}{dm}, \quad (31)$$

then

$$\begin{aligned}
 P(k) & \approx \int dM \frac{dN(M)}{dM} \left(\frac{M_s}{\rho} \right)^2 U(k|M)^2 \\
 & + \int dm \frac{dN_c(m)}{dm} \left(\frac{m}{\rho} \right)^2 u(k|m)^2. \quad (32)
 \end{aligned}$$

In this limit, the total power is well approximated by adding to the power associated with the smooth parent halos the contribution which comes integrating over the subclump mass function.

5 DETAILS

The results presented above are general. When used to model large-scale structure simulations, one will almost always use models of the halo density profiles and halo mass functions which have been found to provide good descriptions of numerical simulations. Specifically, the density profiles F and f are usually described using the functional form given by Navarro, Frenk & White (1997),

$$\frac{\rho(r)}{\bar{\rho}} = \frac{\Delta_{\text{vir}}}{3\Omega} \frac{c^3 f(c)}{(r/r_s)(1+r/r_s)^2} \quad (33)$$

where the profile is truncated at the virial radius r_{vir} , $c \equiv r_{\text{vir}}/r_s$ is called the concentration, and $f(c) = 1/[\ln(1+c) - c/(1+c)]$. The virial radius r_{vir} is defined by requiring that $m = 4\pi r_{\text{vir}}^3 \bar{\rho} \Delta_{\text{vir}}$. For spatially flat universes with $\Omega_0 = (1, 0.3)$ and $\Lambda = 1 - \Omega$, $\Delta_{\text{vir}} = (178, 340)$. The Fourier transform of the density run around such a halo of mass m is

$$\begin{aligned}
 u(k|m) & = f(c) \left[\sin \kappa \left(\text{Si}[\kappa(1+c)] - \text{Si}(\kappa) \right) - \frac{\sin(\kappa c)}{\kappa(1+c)} \right. \\
 & \quad \left. + \cos \kappa \left(\text{Ci}[\kappa(1+c)] - \text{Ci}(\kappa) \right) \right] \quad (34)
 \end{aligned}$$

(Scoccimarro et al. 2001), where $\kappa \equiv kr_{\text{vir}}/c$, $\text{Si}(x) = \int_0^x dt \sin(t)/t$ is the sine integral and $\text{Ci}(x) = -\int_x^\infty dt \cos(t)/t$ is the cosine integral function. The concentration parameter of the halos depends on halo mass; we use the parametrization of this dependence given by Bullock et al. (2001):

$$c(m) \approx \frac{9}{1+z} \left(\frac{m}{m_*(z)} \right)^{-0.1}. \quad (35)$$

The parent halo mass function is well described by

$$\frac{M^2}{\rho} \frac{dN(M, z)}{dM} \frac{dM}{M} = \nu f(\nu) \frac{d\nu}{\nu}, \quad (36)$$

where $\nu \equiv \delta_{\text{sc}}^2(z)/\sigma^2(M)$, ρ is the background mass density, and

$$\nu f(\nu) = A(p) (1 + (q\nu)^{-p}) \left(\frac{q\nu}{2\pi} \right)^{1/2} \exp \left(-\frac{q\nu}{2} \right), \quad (37)$$

with $p \approx 0.3$, $A(p) = [1 + 2^{-p} \Gamma(1/2 - p)/\sqrt{\pi}]^{-1} \approx 0.3222$, and $q \approx 0.75$ (Sheth & Tormen 1999). Here $\delta_{\text{sc}}(z)$ is the critical density required for spherical collapse at z , extrapolated to the present time using linear theory, and

$$\sigma^2(M) = \frac{4\pi}{(2\pi)^3} \int_0^\infty \frac{dk}{k} k^3 P_{\text{Lin}}(k) W^2(kR_0), \quad (38)$$

where $W(x) = (3/x^3)[\sin(x) - x \cos(x)]$ and $R_0 = (3M/4\pi\rho)^{1/3}$. That is to say, $\sigma(M)$ is the rms value of the initial fluctuation field when it is smoothed with a tophat filter of comoving size R_0 , extrapolated using linear theory to the present time. If $p = 1/2$ and $q = 1$, then dN/dM is the same as the universal mass function first written down by Press & Schechter (1974). Note that the mass function is normalized so that

$$\int dM M dN(M)/dM = \rho. \quad (39)$$

The subclump distribution is less well constrained. Therefore, we will consider two models. The first is motivated by the results of numerical simulations (Tormen et al. 1998; Ghigna et al. 1999) which suggest that, on average, a power law in mass is a reasonable model of the typical subclump mass function:

$$\frac{dn(m|M)}{dm} dm = N_0 \left(\frac{M}{m} \right)^\mu \frac{dm}{m} \quad \text{where} \quad \mu < 1, \quad (40)$$

and N_0 is a normalization constant which is set by the fraction of mass in subclumps:

$$\frac{M_{\text{cl}}}{M} = \int_0^M dm \frac{m}{M} \frac{dn(m|M)}{dm} = \frac{N_0}{1-\mu}.$$

In this model, although the total number of subclumps may diverge, the mass contained in them does not. The mean

square subclump mass, which is related to the total number of subclump pairs is

$$M^2 \int_0^M dm \left(\frac{m}{M}\right)^2 \frac{dn(m|M)}{dm} = M^2 \frac{N_0}{2-\mu} = M_{cl} M \frac{1-\mu}{2-\mu}.$$

Simulations suggest $\mu \approx 0.9$ and $M_{cl}/M \approx 0.1$. If $P_{Lin}(k) \propto k^n$ and we use the Press–Schechter form for dN/dM , then in this power law subclump model, the subclump mass function is

$$\frac{m^2}{\rho} \frac{dN_c(m)}{dm} = \frac{2^{(\mu-1)/\alpha}}{\Gamma(1/2)} \left(\frac{M_*}{m}\right)^{\mu-1} \times \Gamma\left(\frac{1}{2} + \frac{\mu-1}{\alpha}, \frac{(m/M_*)^\alpha}{2}\right), \quad (41)$$

where $\alpha = (n+3)/3$ (the value $n \approx -3/2$ is a reasonable approximation to most CDM models). At small masses, $m/M_* \ll 1$, the subclump mass function is a power law: $dN_c/dm \propto m^{-\mu-1}$, whereas at $m/M_* \gg 1$ it drops exponentially.

In practice, the simulations only have finite mass resolution, so a power law model with a minimum mass cutoff may be more appropriate. A low-mass cutoff may also be a useful model if one is only interested in subclumps which could host galaxies. In this case, the mass fraction in subclumps is

$$\frac{M_{cl}}{M} = \int_{M_{min}}^M dm \frac{m}{M} \frac{dn(m|M)}{dm} = N_0 \frac{1 - (M_{min}/M)^{1-\mu}}{1-\mu}.$$

The lower mass cutoff means that the number of subclumps no longer diverges:

$$N_{cl} = \int_{M_{min}}^M dm \frac{dn(m|M)}{dm} = N_0 \frac{(M/M_{min})^\mu - 1}{\mu}.$$

Therefore, when $M_{min} \ll M$, the first term is the dominant one, and the number of subclumps increases as a power law in M . In practice, μ is sufficiently close to unity that the mass fraction in subclumps is approximately $N_0/(1-\mu)$ only for the most massive halos.

Our second model of $dn(m|M)/dm$ is to assume that it is given by the progenitor distribution at some higher redshift z_1 , and all progenitors lost the same fraction of mass as they fell into the parent they now occupy, so they are all a fraction f of the mass they were at z_1 . In this case,

$$\frac{dN_c(m, z_0)}{dm} = \int_{m/f}^\infty dM \frac{dN(M, z_0)}{dM} \frac{dn(m/f, z_1|M, z_0)}{dm}. \quad (42)$$

Mass conservation means that this integral reduces to the mass function at the higher redshift: $dN_c(m, z_0)/dm = dN(m/f, z_1)/dm$. The total amount of mass in these subclumps is

$$\int dm m dN_c(m)/dm = f \int dm (m/f) dN(m/f)/dm = f\rho.$$

This provides a convenient way of thinking about the subclump mass function. In practice, it is likely that the subclumps which have survived to the present come from a distribution of earlier epochs, rather than a single epoch z_1 , and the distribution of z_1 might peak at different redshifts for different values of m/M . Ignoring this subtlety, which is what the model above does, should be a reasonable approximation if the distribution around the mean z_1 is not

broad. In practice, for small values of m/M , the subclump mass function is reasonably well approximated by a power law, and so this model also gives a subclump mass function which is in reasonable agreement with the simulations.

The virtue of this model is that it allows a simple estimate of the shape of the correlation function in the limit in which the subclumps are each a small fraction of the mass of the parent halo, and the total mass in subclumps is a small fraction of the total mass. Recall that, in this limit, the total correlation function is well approximated by the sum of two terms. The first term is the contribution from pairs which are from the smoothly distributed component, and the second is from the subclumps. The subclump contribution, then, can be determined by rescaling the contribution from the smooth component at z_1 . If the particles which were stripped from the halos present at z_1 were random particles, then the number of pairs is lower by a factor of f^2 ; since the halos at z_1 were a factor of $(1+z_1)^3$ denser, the contribution to the correlation function is different by a factor of $f^2(1+z_1)^3$. This yields a factor which is probably slightly smaller than unity. On the other hand, if the mass was stripped from the earlier halos in shells, much like layers off an onion, as simulations suggest, then a better model of the subclump contribution is to truncate the halos which were present at z_1 at a fraction $\sim f$ of their virial radii when estimating how the number of pairs changes with scale. Although this changes the actual shape of the correlation function (e.g., the subclump pairs are shifted to scales which are a factor of f smaller), the typical factor by which the correlations are affected is $f^{-1}(1+z_1)^3$, which can be considerably larger than unity.

6 DISCUSSION

We have shown how to incorporate the effects of substructure into the halo model description of the nonlinear density field. Accounting for this substructure is important on scales smaller than the virial radii of typical halos. The effects are more pronounced for statistics which treat the subclumps preferentially, such as the power spectrum measured in studies of weak galaxy–galaxy gravitational lensing. Substructure will also change the dynamics within halos. Although we have not done so here, it is straightforward to insert our model for substructure into the halo model of the cosmic virial theorem, and the mean pairwise velocity and velocity dispersion developed in Sheth et al. (2001).

The stable clustering limit is a physically appealing description of clustering on small scales (Peebles 1980). It has been argued that a model with smooth halos is inconsistent with this limit (Ma & Fry 2000; Scoccimarro et al. 2001). Substructure changes the shape of the small scale power spectrum (c.f., Fig. 1); at least in principle, it can bring the halo model predictions into agreement with the stable clustering solution. However, it is not obvious that stable clustering is, indeed, the correct physical limit. Smith et al. (2002) argue that the stable clustering assumption is inconsistent with the results of high resolution numerical simulations. They also find that the simulations do not follow the small scale scaling predicted by models in which halos are smooth. Once an accurate model of the subclump mass function is available, it will be interesting to compare the

predictions of our description of substructure with their results.

Although we have focussed primarily on the implications of substructure for the halo model of nonlinear clustering, our results have a wide range of other applications. For example, excess power in the Fourier transforms of images of galaxies or distant clusters can be used to infer the existence of spiral arms or substructure. This is the subject of work in progress. Closely related is the question of what images of high redshift galaxies may look like. Observations through a filter which has a fixed wavelength range probe the emission from high redshift galaxies at shorter restframe wavelengths than for galaxies at low redshift. If obscuration by dust is not a problem, and the UV luminosity is dominated by patchy star forming regions, then the images of high redshift galaxies should show considerable substructure. Our results suggest that, in this case, the power spectrum obtained by Fourier transforming the image of a high redshift patch of sky should show an increase in small scale power.

In addition, although we have phrased the entire discussion of substructure in terms of spatial statistics, this is not really necessary. Large databases describing various observed characteristics of galaxies are now becoming available (e.g., the 2dFGRS and SDSS surveys). If some of n observables are correlated with others, the data will not fill the full n -dimensional space available: the data set itself can be thought of as being clumpy, and the various clumps in dataspace may themselves have substructure. The formalism developed here provides a way of discovering, quantifying and modelling such substructure.

We thank Masahiro Takada for helpful discussions. B.J. acknowledges financial support from a NASA-LTSA grant and a Keck foundation grant.

REFERENCES

- Cooray A., Sheth R. K., 2002, Phys. Rep., in press
 Ghigna S., Moore B., Governato F., Lake G., Quinn T., Stadel J., 2000, ApJ, 544, 616
 Ma C. P., Fry J. N., 2000, ApJ, 543, 503
 McClelland J., Silk J., 1977, ApJ, 217, 331
 Moore B., Quinn T., Governato F., Stadel J., Lake G., 1999, MNRAS, 310, 1147
 Navarro J., Frenk C., White S. D. M., 1997, ApJ, 490, 493
 Neyman J., Scott, E. L., 1952, ApJ, 116, 144
 Peacock J., Smith R., 2000, MNRAS, 318, 1144
 Peebles P. J. E., 1974, ApJ, 189, L51
 Peebles P. J. E., 1980, The Large Scale Structure of the Universe. Princeton Univ. Press, Princeton
 Press W., Schechter P., 1974, ApJ, 187, 425
 Scherrer R.J., Bertschinger E., 1991, ApJ, 381, 349
 Seljak U., 2000, MNRAS, 318, 203
 Scoccimarro R., Sheth R. K., Hui L., Jain B., 2001, ApJ, 546, 20
 Smith R. E., Peacock J. A., Jenkins A., White S. D. M., et al., 2002, MNRAS, submitted, astro-ph/0207664
 Sheth R. K., Jain B., 1997, MNRAS, 285, 231
 Sheth R. K., Lemson G., 1999, MNRAS, 304, 767
 Sheth R. K., Tormen G., 1999, MNRAS, 308, 119
 Sheth R. K., Hui L., Diaferio A., Scoccimarro R., 2001, MNRAS, 325, 1288
 Takada M., Jain B., 2002, MNRAS, submitted, astro-ph/0205055

Tormen G., Diaferio A., Syer D., 1998, MNRAS, 299, 728